

## **VIII- II -1. Project Research**

### **Project 9**

H. Yamana

Research Reactor Institute, Kyoto University

### 1. Objectives and Allotted Research Subjects

Studies on actinide nuclides with careful management are being more important for reprocessing, disposal, partitioning, and transmutation processes in the nuclear fuel cycle. Hot laboratory of KURRI is one of core facilities in Japan, in which actinides especially transuranic elements (Pu, Am, Cm, and so on) can be treated. In our series of past research projects, separation, purification, and synthesis procedures were found to be effective for other elements, for example, rare metal refining. In this context, the actinide studies are expanded for fundamental and application studies on f-elements. Allotted research subjects are as the followings.

- ARS-1 Molecular dynamics simulation of molten salts containing f-elements (N. Ohtori *et al.*)
- ARS-2 Assessment study on chemical properties of actinides in molten salts (M. Myochin *et al.*)
- ARS-3 Absorption spectrophotometric study on titanium in molten salts. (T. Uda *et al.*)
- ARS-4 Study on complexation of actinides in aqueous solutions (T. Sasaki *et al.*)
- ARS-5 Spectroelectrochemical analysis of actinide ions in molten salts and hydrate melts (A. Uehara *et al.*)
- ARS-6 Study on chemical isotope effect of actinides and fission product elements (T. Fujii *et al.*)
- ARS-7 Systematic study on bonding characteristics of trivalent actinides with ligands (A. Shinohara *et al.*)
- ARS-8 Electrochemical study of uranium in pyrochemical reprocessing system (Y. Sakamura *et al.*)
- ARS-9 XAFS analysis on halogenides containing actinides and FP elements (H. Matsuura *et al.*)
- ARS-10 Fundamental and application studies on effective use of f-elements (Y. Ikeda *et al.*)
- ARS-11 Fundamental study on electrolytic formation/dissolution of f-element compounds in molten salts (T. Goto *et al.*)
- ARS-12 Study on neutron capture cross sections of long-lived nuclides by activation method (S. Nakamura *et al.*)

### 2. Main Results and Contents

ARS-1, 2, 3, 8, 9, and 11 studied the chemical behavior of actinides, lanthanides, FP elements, and structural material elements in molten salts, the results of which are to be dedicated to the development of nuclear fuel cycle or general industrial use. MD calculations of LiCl-KCl containing small amount of TbCl<sub>3</sub> was performed in ARS-1 and the structural information around Tb ions was obtained. In ARS-2, reduction from UO<sub>2</sub><sup>2+</sup> to UO<sub>2</sub><sup>+</sup> or U<sup>4+</sup> in alkali chloride melts was studied. An applicability of tungsten as a reductant was confirmed. ARS-3 studied the effect of fluoride ion and oxide ion on the Ti<sup>3+</sup> dissolved in chloride molten salt using the method for development of coherent electrodeposition of Ti<sup>0</sup>. ARS-8 studied the reduction rate of UO<sub>2</sub> in LiCl and discussed the reduction mechanism of UO<sub>2</sub> using an one-dimensional diffusion layer model. In ARS-9, the local structure of Nd ions in molten chlorides was studied by extended X-ray absorption fine structure (EXAFS). All the samples were prepared at KURRI and XAFS analysis was performed at BL11XU, SPring-8. ARS-11 studied electrochemical behavior of Al ion in molten LiCl-KCl and LiCl-KCl-CsCl. The diffusion coefficient of Al(III) was determined. ARS-5 and 10 studied the U chemistry in low temperature or room temperature melts. Coordination circumstance and redox reaction of U ions in Ca chloride hydrate melt was clarified in ARS-5 by spectroscopic and electrochemical methods. In ARS-10, the electrochemical behavior of (EMI)<sub>2</sub>UO<sub>2</sub>Cl<sub>4</sub> (EMI: 1-ethyl-3-methylimidazolium), in the mixture of EMICl and EMIBF<sub>4</sub> was studied and the basic electrochemical data were obtained. ARS-4, 6, and 7 studied aqueous chemistry of actinides and FP elements. ARS-4 studied Th solubility in the presence of humic substances. Dependence of the Th solubility on pH<sub>c</sub> was clarified. ARS-6 studied Sr complexation by ab initio method. Optimized geometries of hydrated Sr species were calculated. ARS-7 studied precipitation properties of the hydroxide complexes of various FP elements. A multitracer produced at KURRI using UO<sub>2</sub> was supplied for ARS-7. Nuclear physical properties of TRUs were investigated in the study, ARS-12. By activation method using KUR, the thermal-neutron capture cross section of <sup>237</sup>Np was newly evaluated.

### 3. Summaries of the achievements

In this research, by using various unique facilities of KURRI for f-element research, new and characteristic chemical and nuclear physical data were obtained. These new information encompass solid chemistry, molten salt and solution chemistry, as well as nuclear reactions of f-elements. The results are useful either for scientific purpose or for technological purpose for nuclear science and general industry.

## PR9-1 Molecular Dynamics Simulation of Molten (Li-K)Cl Containing TbCl<sub>3</sub>

N. Ohtori, Y. Ishii, K. Fukasawa<sup>1</sup>, A. Uehara<sup>1</sup>, T. Fujii<sup>1</sup>, H. Yamana<sup>1</sup> and P. A. Madden<sup>2</sup>

*Department of Chemistry, Niigata University*  
<sup>1</sup>*Research Reactor Institute, Kyoto University*  
<sup>2</sup>*Department of Materials, Oxford University*

**INTRODUCTION:** Molten salts are hopeful solvents for lanthanides and actinides in reprocessing of nuclear fuel. However, knowledge of chemical stability of ionic species in melts is still inadequate to maximize their potential abilities. Information on local structure around ionic species in melts may provide useful measures for their stability in melts. Molecular dynamics (MD) simulation is a powerful tool to elucidate such the structures microscopically. In particular, recent MD simulations with polarizable ionic model (PIM)[1-4] have brought much progress in understanding of structure in ionic melts: they have successfully revealed more reliable pictures of local structures in UCl<sub>3</sub>[2] and LaCl<sub>3</sub>[3] melts and molten alkali chlorides containing LaCl<sub>3</sub>[4] which are comparable with those from XRD and EXAFS studies. In this work, we have performed MD calculations of molten mixtures of lithium and potassium chlorides containing small amount of TbCl<sub>3</sub> in order to obtain the structural information around Tb ions.

**CALCULATIONS:** All the MD calculations have been carried out by using *NVT* condition[5]. The total ion numbers *N* were about 1700 in the cell volume *V* determined from the experimental density[6] at simulated temperature, *T* = 973 K. The ratios of LiCl to KCl in simulated melts were set at 25:75, 50:50, and 75:25 in mol%. Each melt was added with 1 mol% TbCl<sub>3</sub> as a solute. The potential parameters used in the present works were taken from the ref. [7].

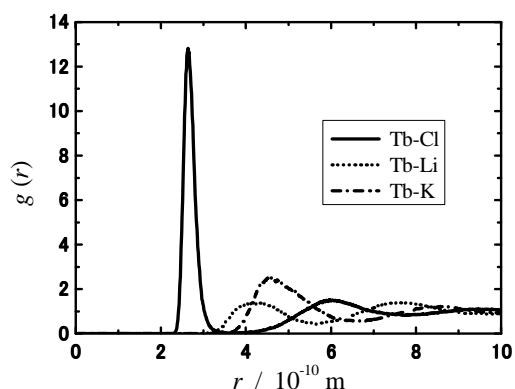


Fig. 1. Radial distribution function, obtained by the MD simulation, between Tb and the other ions in molten (Li-K)Cl at 973 K.

**RESULTS:** Figure 1 shows the obtained radial distribution functions between Tb and the other ions at the ratio of LiCl:KCl = 50:50 mol%. The first peak was observed at 2.64 Å in that for Tb and Cl pair. Although the peak position didn't depend on the composition of solvent melts, the angular distribution function clearly suggests that the first coordinated shell around Tb ion by Cl ions may become more regular octahedron with increasing KCl ratio as illustrated in Fig. 2.

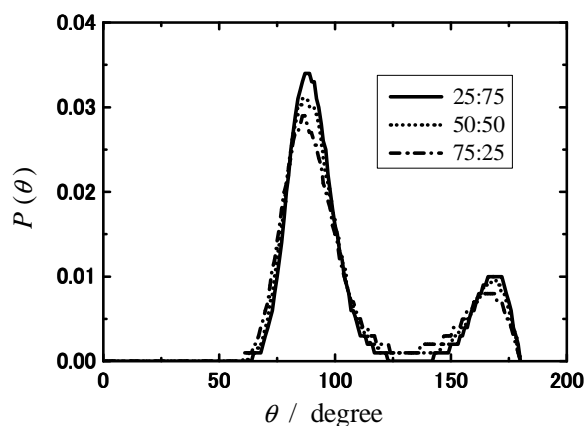


Fig. 2. The calculated angular distribution function of Cl-Tb-Cl in the first coordinated shell around Tb ion in molten (Li-K)Cl at 973 K.

### REFERENCES:

- [1] P. A. Madden, R. Heaton, A. Aguado and S. Jahn, *J. Mol. Struct.:THEOCHEM*, **771** (2006) 9-18.
- [2] Y. Okamoto, P. A. Madden and K. Minato, *J. Nucl. Mater.* 344 (2005) 109-114.
- [3] Y. Okamoto and P. A. Madden *J. Phys. Chem. Solids.*, **66** (2005) 448-451.
- [4] Y. Okamoto, S. Suzuki, H. Shiwaku, A. Ikeda-Ohno, T. Yaita and P. A. Madden, *J. Phys. Chem. A*, **114** (2010) 4664-4671.
- [5] M. P. Allen and D. J. Tildesley, in *Computer Simulation of Liquids*, (Clarendon, Oxford, 1997).
- [6] G. J. Janz, in *NIST Molten Salts Database*, Ver. 2.0, (NIST SRD 27, 1992).
- [7] M. Salanne, C. Simon, P. Turq and P. A. Madden, *J. Phys. Chem. B*, **112** (2008) 1177-1183.

## PR9-2 Reduction from $\text{UO}_2^{2+}$ to $\text{UO}_2^+$ or $\text{U}^{4+}$ in Alkali Chloride Melts by using Tungsten

T. Nagai, A. Uehara<sup>1</sup>, T. Uda<sup>2</sup>, K. Fukasawa<sup>2</sup>, T. Fujii<sup>1</sup>, M. Myochin and H. Yamana<sup>1</sup>

Japan Atomic Energy Agency (JAEA)

<sup>1</sup>Research Reactor Institute, Kyoto University

<sup>2</sup>Graduate School of Engineering, Kyoto University

**INTRODUCTION:** In the pyro-metallurgical method for reprocessing spent oxide fuels, it is necessary to once reduce from those oxides to metallic state. The currently proposed reduction process is electro-reduction technique, which electrolytically reduces  $\text{UO}_2$  and  $\text{PuO}_2$  to their metallic states, and those product metals are dissolved into melt. However, this dissolution is likely to cause appreciable amount of un-reduced oxides, which leads to the formation of actinyl ions dissolved in the melt. Therefore, the reduction of actinyl ions to lower valence states, such as trivalent and tetravalent ions, is desired before the refining operation. In this study, we made researches on the reduction from  $\text{UO}_2^{2+}$  to  $\text{UO}_2^+$  or  $\text{U}^{4+}$  in alkali chloride melts by using tungsten as a reductant.

**EXPERIMENTAL:** All operations were carried out in a glove box filled with dry Ar gas. An anhydrous reagent of LiCl-KCl eutectic was purchased from Aldrich-APL L.L.C. and was used without further treatment. The uranyl source material containing  $\text{UO}_2^{2+}$  was prepared by dissolving the  $\text{U}_3\text{O}_8$  powder with purging dry  $\text{Cl}_2$  gas into the LiCl-KCl eutectic melt. In the spectrum measurements, the reagent of LiCl-KCl eutectic was put into the quartz tube which had a welded optical measurement cell at the bottom of tube. After measuring the background absorption spectrum of the pure melt, a portion of the uranyl source material was added into the melt and the spectrum of  $\text{UO}_2^{2+}$  was measured. And the tungsten mesh was immersed into the melt, and the valence change of uranyl ions was monitored until the spectrum was steady and the changed spectrum was recorded. After then, dry  $\text{Cl}_2$  gas was purged into the melt in presence of the tungsten mesh, and the spectrum was measured after the remaining  $\text{Cl}_2$  in the melt was removed by dry Ar gas purging.

**RESULTS:** In this experiment before the reductive operation, the absorption spectrum of the initial sample of  $\text{UO}_2^{2+}$  in LiCl-KCl eutectic at 500 °C was observed as shown in Fig. 1(a). When the tungsten mesh was immersed into the melt, the spectrum changed and other peaks were observed in the wavenumber range below 23000  $\text{cm}^{-1}$  and small absorptions at 12500 and 15500  $\text{cm}^{-1}$  as shown in Fig. 1(b). This spectrum is agreed with that of  $\text{UO}_2^+$  in LiCl-KCl eutectic.<sup>[1]</sup> This indicates that  $\text{UO}_2^{2+}$  reduced to  $\text{UO}_2^+$  by using the tungsten. However, in the spectrum in Fig. 1(b), the absorption peak of  $\text{U}^{4+}$  at 8500  $\text{cm}^{-1}$  was slightly observed. In a

word, there is a little possibility of the reduction from  $\text{UO}_2^{2+}$  to  $\text{U}^{4+}$ . By  $\text{Cl}_2$  purging into the melt in presence of the tungsten mesh, the absorption peaks of  $\text{UO}_2^{2+}$  and  $\text{UO}_2^+$  decreased and another peaks appeared at 15000, 8500 and 5000  $\text{cm}^{-1}$  as shown in Fig. 1(c). This spectrum was a good agreement with that of  $\text{U}^{4+}$  in LiCl-KCl eutectic.<sup>[2]</sup>

To identify the reductions from  $\text{UO}_2^{2+}$  to  $\text{U}^{4+}$ , these reaction paths were examined. When the tungsten was immersed into the melt, the reduction of  $\text{UO}_2^{2+}$  to  $\text{UO}_2^+$  was observed. This reduction of  $\text{UO}_2^{2+}$  to  $\text{UO}_2^+$  proceeded by the oxidation of tungsten, and can be given by following reaction 1. In the spectrum in Fig. 1(b) which can be slightly observed the peak of  $\text{U}^{4+}$  at 9000  $\text{cm}^{-1}$ , the absorption of the produced  $\text{WCl}_2$  by this reaction 1 was not observed. It is thought that the product of  $\text{WCl}_2$  reacted as following reaction 2. The  $\text{WOCl}_4$  could not be observed in the melt, and seemed to vaporize easily from the melt without remaining. We observed that the volatile compound was coagulated as red powder on the upper area of the cell. After then, purging  $\text{Cl}_2$  into the melt in presence of the tungsten mesh, this coagulated powder grew to be needle-shape crystals on the upper area of the cell. The growth of these crystals was proved to proceed with increasing the amount of  $\text{WOCl}_4$  by the reductions of  $\text{UO}_2^+$  and  $\text{UO}_2^{2+}$  to  $\text{U}^{4+}$  by following reactions 3 and 4, respectively.

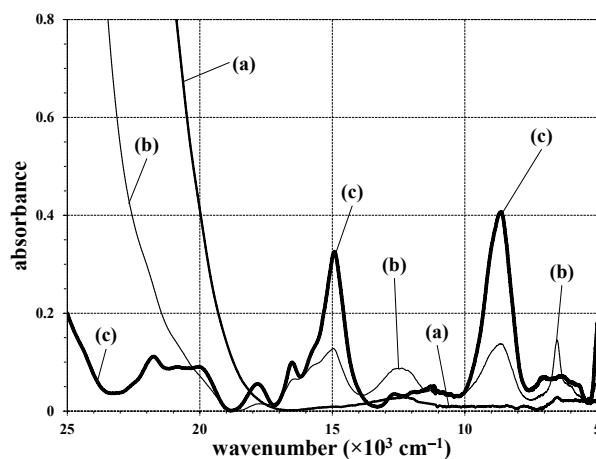
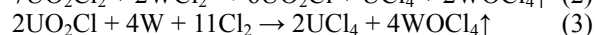
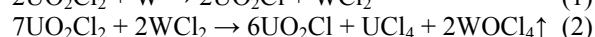
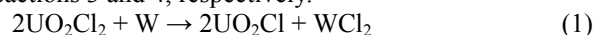


Fig.1. Absorption spectra of uranium ions before tungsten mesh immersion: (a), after tungsten mesh immersion: (b), and after additional dry  $\text{Cl}_2$  gas purging: (c) in LiCl-KCl eutectic at 500 °C.

### REFERENCES:

- [1] D. A. Wenz, *et al.*, *Inorg. Chem.*, **3** (1964) 989-992.  
 [2] G. Landresse, *Anal. Chim. Acta*, **56** (1971) 29-37.

H. Sekimoto, T. Uda<sup>1</sup>, Y. Nose<sup>1</sup>, A. Uehara<sup>2</sup>, T. Fujii<sup>2</sup> and H. Yamana<sup>2</sup>

Department of Materials Science and Engineering, Iwate University

<sup>1</sup>Department of Materials Science and Engineering, Kyoto University

<sup>2</sup>Research Reactor Institute, Kyoto University

## INTRODUCTION:

The information on dissolved ions in molten salt is important for development and optimization of materials processing using molten salt electrolysis. The valence number of electrode active ions is an essential parameter. If active ions are complex ion, the structure of ions (for example, the kind of coordinating ion and its number) is also important. Nagai and his co-workers developed a method for in-situ measurement of absorption spectrum of dissolved ion in high temperature molten salt and applied it to some actinides for development of recycling process for nuclear fuels [1]. This method is useful to investigate the valence number and the complex of dissolved ions in molten salt. In this study, we investigated the effect of fluoride ion and oxide ion on the trivalent titanium ion dissolved in chloride molten salt using the method for development of coherent electrodeposition of metallic titanium.

## EXPERIMENTS:

We measured the absorbance of  $\text{TiCl}_3$  dissolved in NaCl-KCl equimolar molten salt to obtain the absorption spectrum of  $\text{Ti}^{3+}$ . And then, we investigated the effect of  $\text{F}^-$  and  $\text{O}^{2-}$  on  $\text{Ti}^{3+}$  by repeating measurement of absorbance and addition of NaF and  $\text{Na}_2\text{O}$ , respectively. The samples used in this study were mixtures of NaCl, KCl, NaF,  $\text{Na}_2\text{O}$  and  $\text{TiCl}_3$  which were prepared by melting the reagents in a closed stainless container. The titanium trichloride ( $\text{TiCl}_3$ ) was synthesized by the reported technique [2].

## RESULTS:

Figure 1 shows the absorption spectra of the trivalent titanium ion in NaCl-KCl equimolar molten salt at 700 °C. The chloride complex of  $\text{Ti}^{3+}$  has an absorption peak at around 786 nm. We confirmed that the shape of the spectrum was drastically changed by adding  $\text{F}^-$  as shown in Fig. 1 (a). This change gradually proceeded by adding NaF until the ratio of the concentration of  $\text{F}^-$  to that of  $\text{Ti}^{3+}$  ( $C_{\text{F}^-} / C_{\text{Ti}^{3+}}$ ) was over about 6. These results indicate that  $\text{Ti}^{3+}$  dissolved in NaCl-KCl molten salt reacted with  $\text{F}^-$  to form fluoride complex with 6 coordinate ions ( $\text{TiF}_6^{3-}$ ), which may be more stable than chloride complex of  $\text{Ti}^{3+}$ . On the other hand, by adding  $\text{O}^{2-}$ , the shape of the spectrum of  $\text{Ti}^{3+}$  was not changed but the spectrum was

slightly shifted upward as shown in Fig. 1 (b). We considered that this increase of absorbance is due to the decrease of the dissolved  $\text{Ti}^{3+}$  because the molar absorbance shown in Fig. 1 (b) is an apparent value obtained by division of the nominal mole of  $\text{Ti}^{3+}$  by the volume of the molten salt. We also confirmed that black particles were suspended in the molten salt after adding  $\text{O}^{2-}$ . The particles were identified to be  $\text{TiOCl}$  by XRD. Therefore, we considered that when  $\text{O}^{2-}$  is introduced to the NaCl-KCl molten salt containing  $\text{Ti}^{3+}$ ,  $\text{Ti}^{3+}$  reacts with  $\text{O}^{2-}$  and  $\text{Cl}^-$  to form  $\text{TiOCl}$ .

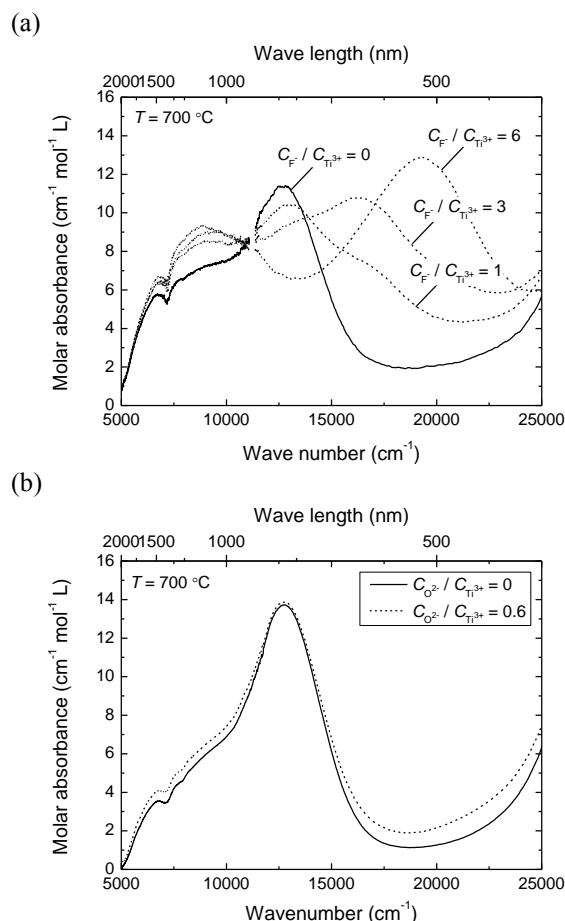


Fig. 1. Absorption spectra of  $\text{Ti}^{3+}$  in NaCl-KCl equimolar molten salt. Solid line attributes the absorption by chloride complex of  $\text{Ti}^{3+}$ . The broken lines corresponds the absorption spectra after adding anion, (a)  $\text{F}^-$  and (b)  $\text{O}^{2-}$ .

## REFERENCES:

- [1] T. Nagai, T. Fujii, O. Shirai and H. Yamana, J. Nuc. Sci. Tech., **41** (2004) 690-695.
- [2] H. Sekimoto, Y. Nose, T. Uda, H. Sugimura, High Temp. Mater. Proc., **30** (2012) 435-440.

T. Sasaki, Y. Matsuura, T. Kobayashi, K. Date, H. Moriyama<sup>1</sup>, T. Fujii<sup>1</sup> and H. Yamana<sup>1</sup>

Department of Nuclear Engineering, Kyoto University  
<sup>1</sup>Research Reactor Institute, Kyoto University

**INTRODUCTION:** The amount of radionuclide potentially mobilized in radioactive waste repository system is related to its solubility in groundwater. For tetravalent actinide, the solubility under relevant geological condition is rather limited because of strong hydrolysis reaction. However, in the presence of inorganic and organic complexing ligands, the ‘apparent’ solubility of tetravalent actinide may be influenced by forming complexes and compounds. For the reliable assessment of their migration behaviour, it is important to clarify dominant species and evaluate the solubility of tetravalent actinide quantitatively. Among various kinds of complexing ligands, humic acid (HA) prevails in groundwater and has strong complexation capability. HA consists of aromatic rings and hydrocarbon chains, has negatively charged functional groups, such as carboxyl and phenolic groups, and would strongly coordinate with tetravalent actinide with these functional groups. In the present study, we investigate the solubility of thorium(IV) in the presence of HA under different pH and ionic strength conditions to evaluate the impact of HA to the solubility of thorium(IV).

**EXPERIMENTAL:** A stock solution of thorium perchlorate was prepared from  $\text{Th}(\text{NO}_3)_4 \cdot 4\text{H}_2\text{O}$  and a stock solution of purified humic acid (Aldrich HA) was obtained after purification. The initial Th concentration of sample solutions was set to be  $10^{-6}$  mol/dm<sup>3</sup> (M) and the initial concentrations of humic acid were set to be from  $5.28 \cdot 10^{-6}$  to  $5.28 \cdot 10^{-3}$  eq/L. The hydrogen ion concentration ( $\text{pH}_c$ ) was adjusted from 4 to 12 with  $\text{HClO}_4/\text{NaOH}$  and the ionic strength ( $I$ ) was adjusted to be 0.1 and 1.0 by adding appropriate amount of  $\text{NaClO}_4$ . The sample solutions were kept in an Ar glove box. After given periods, the  $\text{pH}_c$  of each sample solution was measured using combination glass electrodes (9611-10D Horiba Ltd.) and the supernatant was filtrated through  $0.45 \mu\text{m}$  syringe filter and 3k Da ultrafiltration membranes (ca. 2 nm pore size). Th concentrations after each filtration were determined by ICP-MS (HP4500, Hewlett Packard). The detection limit was around  $10^{-10}$  M.

**RESULTS:** Th solubility in the presence of HA after 144 days is shown in Fig. 1. A dashed curve represents the solubility of  $\text{Th}(\text{OH})_4(\text{am})$  in the absence of HA [1]. In the presence of  $5.28 \cdot 10^{-3}$  eq/L HA, the solubility values after filtration through  $0.45 \mu\text{m}$  remain initial Th concentration level, while those after filtration through 3k Da show considerably low values. This trend is in

good agreement with the size distribution of purified HA itself, and rather different from the size distribution of Th hydrolysis species. Therefore, it is considered that Th forms a complex with HA and the complex was filtered out by 3k Da membranes. In the presence of  $5.28 \cdot 10^{-5}$  eq/L HA, similar trend is shown. In the acidic  $\text{pH}_c$ , the solubility values after filtration through  $0.45 \mu\text{m}$  membranes are slightly lower than those in neutral and alkaline  $\text{pH}_c$ . Under acidic  $\text{pH}_c$  condition, HA is considered to release less protons and agglomerate to form larger species. The Th-HA complex may agglomerate in a similar manner and filtered out even by  $0.45 \mu\text{m}$ . The trend is observed under the condition of  $I = 1.0$  more clearly, suggesting that co-existing cation ( $\text{Na}^+$ ) may affect the agglomeration of HA. Thus, we confirmed that HA coordinate with tetravalent Th to change the ‘apparent’ solubility of  $\text{Th}(\text{OH})_4(\text{am})$ . It is also indicated that size distribution of the Th-HA complex is highly important, since Th-HA complex is thought to increase in size and filtered out by small size filters such as 3k Da membranes under certain condition. For the quantitative discussion of Th solubility in the presence of HA, and evaluation using thermodynamic data, further investigation is needed.

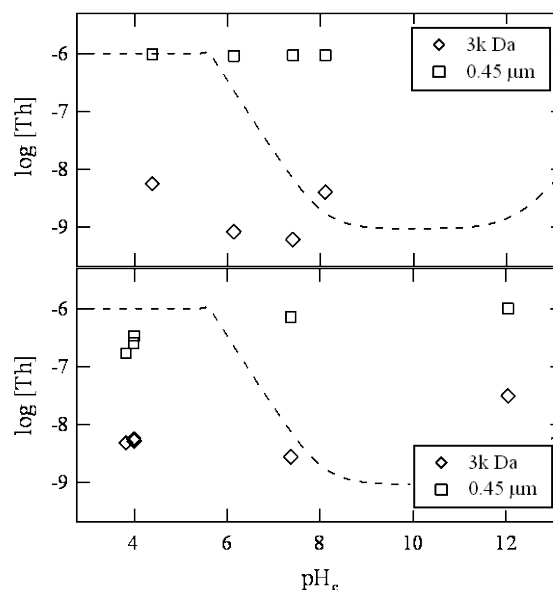


**Fig. 1.** Th solubility in the presence of  $5.28 \cdot 10^{-3}$  eq/L HA (upper) and  $5.28 \cdot 10^{-5}$  eq/L HA (lower) after filtration through  $0.45 \mu\text{m}$  ( $\square$ ) and 3k Da ( $\diamond$ ). The initial Th concentration is  $10^{-6}$  M, and a dashed curve represents the solubility of  $\text{Th}(\text{OH})_4(\text{am})$  in the absence of HA [1].

#### REFERENCES:

[1] Kobayashi, T., Sasaki, T., Takagi, I., Moriyama, H., *J. Nucl. Sci. Technol.* **48** (2011) 993–1003.

## PR9-5 Electrochemical Characteristics of Uranium Ions in Calcium Chloride Hydrate Melts

A. Uehara, T. Nagai<sup>1</sup>, T. Fujii, O. Shirai<sup>2</sup>, N. Sato<sup>3</sup> and H. Yamana

<sup>1</sup> Research Reactor Institute, Kyoto University

<sup>1</sup> Nuclear Fuel Cycle Engineering Lab., Japan Atomic Energy Agency

<sup>2</sup> Graduate School of Agriculture, Kyoto University

<sup>3</sup> Institute of Multidisciplinary Research for Advanced Materials, Tohoku University

### INTRODUCTION:

The calcium chloride hexahydrate,  $\text{CaCl}_2 \cdot 6\text{H}_2\text{O}$ , and similar hydrate melts are of considerable interest as solvents with properties intermediate between those of aqueous solution and molten salts. In view of the activity coefficients, viscosity and structural property, it is considered that water molecules in  $\text{CaCl}_2 \cdot 6\text{H}_2\text{O}$  melts are strongly coordinated to the calcium ion and there are no free water molecules to dissociate to form  $\text{H}^+$  and  $\text{OH}^-$ . As a result, this material has advantages such as inorganic-based melt and low melting temperature. In the present study, coordination circumstance and redox reaction of uranium ions such as  $\text{U}^{4+}$  and  $\text{UO}_2^{2+}$  in  $\text{CaCl}_2 \cdot n\text{H}_2\text{O}$  hydrate melt ( $n = 6 - 10$ ) have been investigated by spectroscopic and electrochemical methods. The chemical behavior of uranium ion in the hydrate melt was compared with that in the other solvents such as high temperature [1] or room temperature [2] molten salts, organic solvents [3] and relatively low concentration solution of hydrochloric acid [4].

### EXPERIMENTAL:

For the electrochemical measurements, a three-electrode system was used. A pyro-graphite carbon (Toyo Tanso Co. Ltd.) of 3 mm diameter was used as a working electrode, and the silver|silver chloride ( $\text{Ag}|\text{AgCl}$ ) electrode was used as a reference electrode. This reference electrode, in which was put an aqueous solution containing 1 M LiCl along with a Ag wire of 1 mm diameter coated by AgCl. For voltammetric operation, the platinum mesh electrode was employed as a counter electrode. Electrochemical measurement systems, Hz-5000 (Hokuto Denko Co.) were used for the cyclic voltammetry and the linear sweep voltammetry. Controlled-potential electrolysis was carried out in order to identify the electrode reaction. In this experiment, a rotating carbon electrode was employed as a working electrode to enhance the efficiency of the electrolysis. The counter electrode was also a platinum mesh electrode, and the counter phase was separated by glass filter membrane from the objective phase to avoid cyclic redox reaction. After the electrolysis, absorption spectra were measured. A self-registering spectrophotometer UV-1000 (Shimadzu Co.) was used for the measurements over the wavelength from 400 to 900 nm.

These measurements were carried out at  $300 \pm 2$  K.

### RESULTS:

Influences of the water content on chemical status of  $\text{UO}_2^{2+}$  and  $\text{U}^{4+}$  in  $\text{CaCl}_2 \cdot n\text{H}_2\text{O}$  were also studied by electrochemical and spectroscopic methods. Visible absorption spectra of  $\text{U}^{4+}$  in  $\text{CaCl}_2 \cdot n\text{H}_2\text{O}$  changed drastically along with the water content. This suggested the strong influence of water content on the coordination status of  $\text{U}^{4+}$  in the melt. Cyclic voltammograms of  $\text{U}^{4+}$  in  $\text{CaCl}_2 \cdot n\text{H}_2\text{O}$  indicated that the  $\text{U}^{4+}/\text{U}^{3+}$  redox couple was quasi-reversible reaction and that the formal redox potential for the  $\text{U}^{4+}/\text{U}^{3+}$  couple was almost independent of the hydration number  $n$  to be  $0.790 \pm 0.010$  V vs.  $\text{Ag}|\text{AgCl}$  reference electrode (1M LiCl) at 298 K. Diffusion coefficients of  $\text{U}^{4+}$  depended not only on the hydration number  $n$  but also on the temperature in the melts. The oxidation peaks of voltammogram were attributed to the oxidation of  $\text{U}^{4+}$  to uranyl ions by the water molecules. The results of the cyclic voltammogram of  $\text{UO}_2^{2+}$  in  $\text{CaCl}_2 \cdot n\text{H}_2\text{O}$  showed that there are various reductions from  $\text{UO}_2^{2+}$  to lower valence states including the formation of  $\text{UO}_2^+$  and solid  $\text{UO}_2$ . The  $\text{UO}_2^+$  formed in  $\text{CaCl}_2 \cdot 6\text{H}_2\text{O}$  was identified spectrophotometrically after the controlled potential electrolysis. On the other hand, it is reported that  $\text{UO}_2^+$  formed electrochemically in diluted acidic solutions such as 0.1M HCl disproportionates spontaneously to form  $\text{U}^{4+}$  and  $\text{UO}_2^{2+}$ . These results indicate that the  $\text{UO}_2^+$  in  $\text{CaCl}_2 \cdot 6\text{H}_2\text{O}$  was more stable than that in the acidic solutions. It was also found that  $\text{UO}_2^+$  disproportionated to form  $\text{UO}_2^{2+}$  and  $\text{UO}_2$  in  $\text{CaCl}_2 \cdot 6\text{H}_2\text{O}$ .

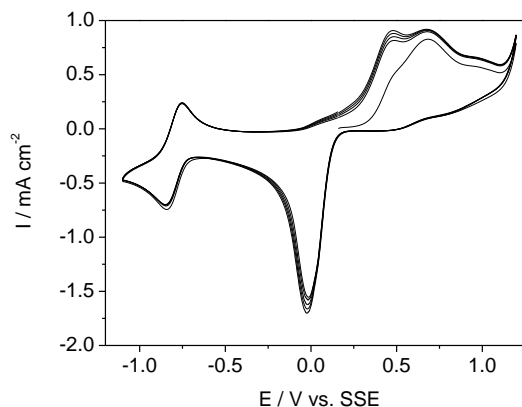


Fig. 1. Cyclic voltammogram of  $\text{U}^{4+}$  in  $\text{CaCl}_2 \cdot 6\text{H}_2\text{O}$  containing 0.05 M  $\text{UCl}_4$ . Potential scanning rate is  $0.02 \text{ V s}^{-1}$ .

### REFERENCES:

- [1] T. Nagai, A. Uehara, T. Fujii, O. Shirai, N. Sato, H. Yamana, *J. Nucl. Sci. Technol.*, 42 (2005) 1025.
- [2] P. Giridhar, K.A. Venkatesan, T.G. Srinivasan, P.R. Vasudeva Rao, *Electrochim. Acta*, 52 (2007) 3006.
- [3] L. Martinot, D. Laeckmann, L. Lopes, T. Materne, V. Muller, *J. Alloys Compd.*, 185 (1992) 151.
- [4] W.E. Harris, I.M. Kolthoff, *J. Am. Chem. Soc.*, 69 (1947) 446.

T. Fujii, S. Fukutani and H. Yamana,

Research Reactor Institute, Kyoto University

**INTRODUCTION:** Strontium 90 ( $^{90}\text{Sr}$ ) is known as one of fission products, and it has a large fission yield. In order to know the chemical behavior of Sr complexes, we study the highly precise isotopic analysis of Sr [1]. The analytical technique will be helpful to understand the fractionation mechanism of Sr isotopes in environmental samples and so on. In parallel with the analytical studies, quantum chemical calculations are performed to check the validity of analytical results. The equilibrium constant of the isotope exchange reaction can be theoretically obtained as the reduced partition function ratio (RPFR) of isotopologues. The RPFR value is usually calculated through harmonic vibration analysis. In this study, we report some *ab initio* calculations of hydrated  $\text{Sr}^{2+}$  complexes.

**COMPUTATIONAL DETAILS:** The orbital geometries and vibrational frequencies of hydrated Sr(II) complexes were calculated by using the conventional Hartree-Fock (HF) approximation and the density functional theory (DFT) as implemented by the Gaussian03 code [2]. The DFT method employed here is a hybrid density functional consisting of Becke's three-parameter non-local hybrid exchange potential (B3) with Lee-Yang-and Parr (LYP) non-local functionals (B3LYP). The 6-31++G\*\* basis set was chosen for H and O, and LanL2DZ was chosen for Sr. The former is an all-electron basis, while the latter is an effective core potential (ECP) basis.

**RESULTS:** The hydrated  $\text{Sr}^{2+}$  species is generally thought to be present as eight-coordinated  $\text{Sr}(\text{H}_2\text{O})_8^{2+}$ . The structure was converged to be the square antiprism with 2.69 Å Sr-O bond length [3]. This agreed with literature data determined by a combination of the extended X-ray absorption fine structure (EXAFS) spectrometry and molecular dynamics (MD) [4]. Isotope fractionation of a Sr carbonate complex shown in Fig. 1 was estimated in the present study. The coordination number was set to be eight. Carbonate ion was treated as a bidentate ligand. This model complex was unstable and deformed into  $[\text{SrCO}_3(\text{H}_2\text{O})_5]\text{H}_2\text{O}$  with the 6th water molecule moving out of the inner coordination shell.

The isotope enrichment factor due to the intramolecular vibrations can be evaluated from RPFR [5],  $(s/s')f$ ,

$$\ln (s/s')f = \Sigma[\ln b(u_i') - \ln b(u_i)] \quad (1)$$

where

$$\ln b(u_i) = -\ln u_i + u_i/2 + \ln (1 - e^{-u_i}) \quad (2)$$

and

$$u_i = hv_i/kT \quad (3)$$

$v$  stands for vibrational frequency. The subscript  $i$  stands for the  $i$ th molecular vibrational level with primed variables referring to the light isotopologue. The isotope en-

richment factor due to the molecular vibration can be evaluated from the frequencies ( $v$ ) summed over all the different modes.

The  $\ln(s/s')f$  values of hydrated Sr(II) species were estimated by quantum chemical calculations. The results are shown in Table 1. Carbonate showed larger  $\ln(s/s')f$  value compared with that of the hydrated Sr ion. This suggests that heavier Sr isotopes enrich in carbonate. These values may be useful to estimate the degree of isotope fractionation.

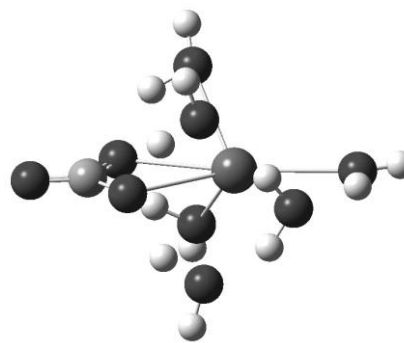


Fig. 1. Equilibrium geometry of  $\text{SrCO}_3(\text{H}_2\text{O})_6$ .

Table 1  $\ln(s/s')f$  (‰) of hydrated  $\text{Sr}^{2+}$  species for an isotope pair,  $^{86}\text{Sr}$ - $^{88}\text{Sr}$ .

	HF	B3LYP
$\text{Sr}(\text{H}_2\text{O})_8^{2+}$	1.424	1.416
$\text{SrCO}_3(\text{H}_2\text{O})_6$	1.640	1.507

#### REFERENCES:

- [1] T. Fujii *et al.*, KURRI Prog. Rep. 2007 (2008) 93-93.
- [2] M. J. Frisch *et al.*, Gaussian 03 Revision B.05, Gaussian Inc., Pittsburgh PA, 2003.
- [3] T. Fujii *et al.*, KURRI Prog. Rep. 2008 (2009) 99-99.
- [4] L. X. Dang *et al.*, J. Phys. Chem., **107** (2003) 14119-14123.
- [5] J. Bigeleisen and M. G. Mayer, J. Chem. Phys., **15** (1947) 261-267.



## PR9-7 Investigation on the Properties of Hydroxide Precipitation Using KUR Multitracer

Y. Kasamatsu, N. Shiohara, T. Yokokita, Y. Komori, T. Yoshimura, N. Takahashi, K. Takamiya<sup>1</sup>, and A. Shinohara

Graduate School of Science, Osaka University  
<sup>1</sup>Research Reactor Institute, Kyoto University

**INTRODUCTION:** Chemistry researches on actinide and transactinide elements at the uppermost end of the periodic table are very important in inorganic chemistry. It is because the chemical properties of these elements would be unique, which is caused by strong relativistic effect on the shell electrons. It is, however, difficult to perform chemical experiment with heavy actinide and transactinide elements because these must be produced at accelerators using heavy-ion induced nuclear reactions with low production rates. Furthermore, these elements have short half-lives. Thus, we need to establish new experimental methods or apparatuses specified for these elements and test them using the elements whose chemical properties are known.

We have ever developed the preparation method of a coprecipitate sample with Sm which has high energy resolution in the  $\alpha$  spectrometry by using membrane filters [1]. In this work, precipitation properties of the hydroxide complexes of various elements were studied by this method using multitracer produced with Kyoto University Reactor (KUR) aiming at the precipitation experiment of heavy actinide and transactinide elements.

**EXPERIMENTS:** The KUR multitracer sample was prepared by irradiating thermal neutrons on  $\text{UO}_2$  powder which is mixed with NaCl at KUR [2]. Fission products implanted in NaCl were dissolved in 0.01 M HCl and were separated from the  $\text{UO}_2$  powder by a suction filtration. A portion of the sample was subjected to  $\gamma$ -ray measurement by a Ge detector, and count rates of  $\gamma$ -ray peaks and their time dependences were measured.

In the precipitation experiment, 200  $\mu\text{L}$  of water and 20  $\mu\text{L}$  (20  $\mu\text{g}$ ) of Sm standard solution (1 M  $\text{HNO}_3$ ) were added into 20–40  $\mu\text{L}$  of the multitracer solution. After mixing it, 2 mL of basic solution was added to generate hydroxide precipitate. In the present experiment, we used dilute  $\text{NH}_3$  solution, concentrated  $\text{NH}_3$  solution, 0.1, 1, 6, and 12 M NaOH solutions as the basic solutions to observe the dependence of the precipitation yield on the component of the basic solution. Subsequently, the solution was stirred for 10 s and was soon filtrated with a polypropylene membrane filter. To check the complete precipitation of the samples, precipitate samples with stirring for 5 min in water bath after adding the basic solutions were also prepared. The samples were then dried on heater at 100 degree C and were assayed for  $\gamma$ -ray

measurements. Supernatant solutions were evaporated to dryness and were also subjected to measurements. The precipitation yields were determined from the results of the  $\gamma$ -ray measurements.

**RESULTS:** Main nuclides identified from the  $\gamma$ -ray energies and their half-lives were  $^{24}\text{Na}$ ,  $^{91}\text{Sr}$ ,  $^{95,97}\text{Zr}$ ,  $^{99}\text{Mo}$ ,  $^{103}\text{Ru}$ ,  $^{105}\text{Rh}$ ,  $^{131\text{m},132}\text{Te}$ ,  $^{131,133}\text{I}$ ,  $^{140}\text{Ba}$ ,  $^{140}\text{La}$ ,  $^{141,143}\text{Ce}$ , and  $^{151}\text{Pm}$ . To obtain correct precipitation yields, we exclude the nuclides whose decays are affected by their parent or daughter nuclide from determining the yields.

The precipitation yield for each nuclide is shown in Table 1. The yields of alkaline metal element were almost 0 %, and those of lanthanide elements were almost 100 %. It would indicate that chemical properties which are inherent in each element influence the coprecipitation yields with Sm. For some elements such as Zr and Ru, interesting dependences of the yields on the component of the basic solution were observed. For further discussion, precipitation properties of these elements, not coprecipitation properties, should be studied.

Table 1. Precipitation yields of multitracer.

Nuclide	dil. $\text{NH}_3$	conc. $\text{NH}_3$	0.1M NaOH
Na-24	0.1 $\pm$ 0.0	0.0 $\pm$ 0.0	0.0 $\pm$ 0.0
Sr-91	43.3 $\pm$ 0.8	74.6 $\pm$ 1.2	5.6 $\pm$ 0.2
Zr-97	100.0 $\pm$ 3.7	100.0 $\pm$ 15.6	100.0 $\pm$ 0.8
Ru-103	89.0 $\pm$ 9.9	50.7 $\pm$ 6.9	98.1 $\pm$ 5.7
Rh-105	100.0 $\pm$ 0.8	60.8 $\pm$ 1.2	100.0 $\pm$ 1.0
Te-132	79.8 $\pm$ 5.6	68.4 $\pm$ 0.6	95.4 $\pm$ 0.7
I-131	16.0 $\pm$ 0.6	9.9 $\pm$ 0.5	8.2 $\pm$ 0.2
I-133	20.5 $\pm$ 0.3	18.4 $\pm$ 0.3	11.8 $\pm$ 0.1
Ba-140	15.2 $\pm$ 1.9	100.0 $\pm$ 1.0	2.6 $\pm$ 0.0
Ce-143	100.0 $\pm$ 1.1	100.0 $\pm$ 1.1	100.0 $\pm$ 1.0
Pm-151	100.0 $\pm$ 1.5	100.0 $\pm$ 1.4	100.0 $\pm$ 24.3

	1M NaOH	6M NaOH	12M NaOH
Na-24	0.0 $\pm$ 0.0	0.2 $\pm$ 0.1	0.2 $\pm$ 0.0
Sr-91	1.3 $\pm$ 0.1	0.0 $\pm$ 0.0	0.0 $\pm$ 0.0
Zr-97	84.2 $\pm$ 5.1	-	-
Ru-103	82.6 $\pm$ 4.2	15.2 $\pm$ 0.6	9.0 $\pm$ 0.3
Rh-105	100.0 $\pm$ 1.7	77.2 $\pm$ 2.4	74.5 $\pm$ 2.0
Te-132	35.1 $\pm$ 0.5	32.1 $\pm$ 1.4	23.5 $\pm$ 0.7
I-131	1.4 $\pm$ 0.1	1.7 $\pm$ 0.1	3.1 $\pm$ 0.1
I-133	4.0 $\pm$ 0.0	3.7 $\pm$ 0.2	5.9 $\pm$ 0.2
Ba-140	0.0 $\pm$ 0.0	0.1 $\pm$ 0.0	0.1 $\pm$ 0.0
Ce-143	100.0 $\pm$ 1.7	100.0 $\pm$ 2.8	100.0 $\pm$ 2.2
Pm-151	100.0 $\pm$ 12.4	100.0 $\pm$ 16.0	100.0 $\pm$ 28.3

### REFERENCES:

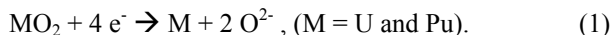
- [1] H. Kikunaga *et al.*, Appl. Radiat. Isot., **67** (2009) 539-543.
- [2] K. Takamiya *et al.*, J. Nucl. Radiochem. Sci., **1** (2000) 81-82.

## PR9-8 Mechanism of Electrolytic Reduction of $\text{UO}_2$ Pellet in Molten LiCl and LiCl-KCl

Y. Sakamura, M. Iizuka, T. Fujii<sup>1</sup>, A. Uehara<sup>1</sup> and H. Yamana<sup>1</sup>

Central Research Institute of Electric Power Industry  
<sup>1</sup>Research Reactor Institute, Kyoto University (KURRI)

**INTRODUCTION:** The electrolytic reduction process of actinide oxides in molten LiCl salt bath at 923 K has been developed for the nuclear fuel reprocessing.  $\text{UO}_2$  and MOX can be reduced to the metallic form by the following cathode reaction:



Since salt-soluble FPs of alkali and alkaline-earth metals accumulate in the LiCl, their effect on  $\text{UO}_2$  reduction was experimentally studied at KURRI [1].  $\text{UO}_2$  pellets were reduced by potential-controlled electrolysis in various LiCl salt baths containing up to 30 mol% of KCl. The reduction progressed from the outside toward the center of the  $\text{UO}_2$  pellet. It was found that the reduction rate was remarkably decreased after the additions of KCl, which was attributed to the decrease in the solubility of  $\text{Li}_2\text{O}$  in the salt bath with increasing the KCl concentration [2]. In this study, the reduction mechanism of  $\text{UO}_2$  was discussed using an one-dimensional diffusion layer model.

**CALCULATION MODEL:** The reduction mechanism of  $\text{UO}_2$  pellets is considered as follows. The diffusion of  $\text{O}^{2-}$  ions from the inside of  $\text{UO}_2$  pellet to the bulk salt determined the reduction rate. At first, the surface of  $\text{UO}_2$  pellet is reduced to metal. The reduced U metal layer has gaps because the density of  $\text{UO}_2$  is about 60% that of U metal, and the molten salt then permeates into the gaps. The  $\text{O}^{2-}$  ionized at the U metal/ $\text{UO}_2$  interface is discharged to the bulk salt through the molten salt pass by diffusion. The  $\text{O}^{2-}$  concentration seems to be the solubility limit at the vicinity of the U metal/ $\text{UO}_2$  interface since charge transfer of Eq. (1) is fast at high temperature. Therefore, the  $\text{O}^{2-}$  solubility to determine the driving force of diffusion strongly affects the reduction rate.

To simulate how the reduction progresses, an one-dimensional diffusion layer model was designed as shown in Fig. 1. The assumptions are as follows.

- The cathode potential is negative enough to reduce  $\text{UO}_2$  to U metal and charge transfer is fast. Thus, the diffusion of  $\text{O}^{2-}$  through the salt is the rate determining step.
- The U metal formed in the beginning of electrolysis shrinks to give a dense outer layer,  $L_1$  [1]. Inside the dense outer layer, the volume shrinkage of U metal does not occur to give a porous inner layer,  $L_2$ .  $\phi_1$  and  $\phi_2$  are effective porosities of  $L_1$  and  $L_2$ , respectively.
- In the  $\delta_2$  layer next to the  $\text{UO}_2$ /U metal interface, the value of diffusion coefficient of  $\text{O}^{2-}$ ,  $D_1$ , might be smaller than the value at a low concentration,  $D_0$ , because the viscosity would increase with increasing the  $\text{O}^{2-}$  concentration. There is a diffusion layer,  $\delta_1$ , outside of  $L_1$ .

Then, the following equation can be derived from the mass balance of  $\text{O}^{2-}$  ions.

$$\frac{i}{2F} = D_1 \phi_2 \frac{C_0 - C_1}{\delta_2} = D_0 \phi_2 \frac{C_1 - C_2}{L - L_1 - \delta_2} = D_0 \phi_1 \frac{C_2 - C_3}{L_1} = D_0 \frac{C_3 - C_4}{\delta_1} \quad (2)$$

Here,  $i$  is the current density,  $F$  is the Faraday constant and  $C_i$  is the concentration of  $\text{O}^{2-}$  at each interface.

**RESULTS AND DISCUSSION:** The relationship between the thickness of U metal layer and square root of the electrolysis time was calculated for LiCl and LiCl-10mol% KCl systems using Eq. (2) and the values of parameters appropriately determined considering the literature [1, 2]. Fig. 2 shows the calculated results along with the experimental results [1]. The values of  $D_0$  for LiCl-10mol%KCl,  $\phi_1$  and  $\phi_2$  were mainly adjusted to best fit the experimental results. The negative deviation from the parabolic relation was reproduced by assuming both the shrinkage of outer U metal layer and the smaller diffusion coefficient of  $\text{O}^{2-}$  in a high concentration range. For improving the simulation, it is strongly desired to clarify the dependence of diffusion coefficient of  $\text{O}^{2-}$  on KCl and  $\text{O}^{2-}$  concentrations as well as the configuration of pore in U metal products.

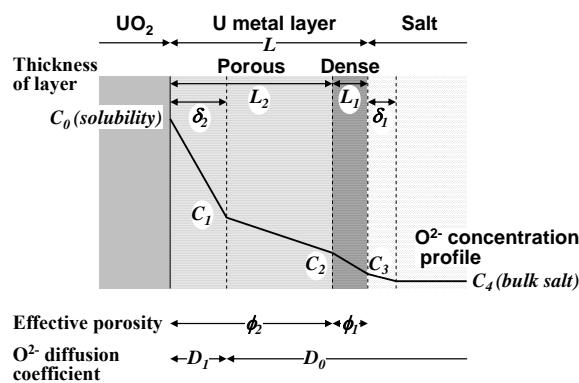


Fig. 1. Schematic view of one-dimensional diffusion layer model for electrolytic reduction of an  $\text{UO}_2$  pellet.

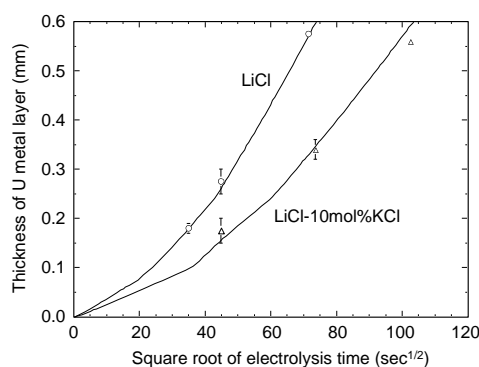


Fig. 2. Dependence of thickness of U metal layer on electrolysis time: comparison of calculated results (solid lines) with experimental values [1].

### REFERENCES:

- Y. Sakamura, J. Nucl. Mater., **412** (2011) 177.
- Y. Sakamura, J. Electrochem. Soc., **157** (2010) E135.

## PR9-9 Local Structural Analysis of Neodymium Cation in Molten Various Chlorides

H. Matsuura, A. Nezu, T. Yaita<sup>1</sup>, H. Shiwaku<sup>1</sup>, H. Yamana<sup>2</sup>, T. Fujii<sup>2</sup>, K. Fukasawa<sup>2</sup>, T. Uda<sup>2</sup> and A. Uehara<sup>2</sup>

Research Laboratory for Nuclear Reactors, Tokyo Institute of Technology

<sup>1</sup>Kansai Photon Institute, JAEA

<sup>2</sup>Research Reactor Institute, Kyoto University

**INTRODUCTION:** It is very essential to grasp the chemical behaviour of fuel elements and fission products in each step of processes in order to make realization of pyrochemical reprocessing of nuclear fuel. Neodymium is one of the fission products as well as the rare earth element having divalent cation through the electrochemical reaction[1]. It seems to be existing the simple relationship between the structural model and electrochemical properties of molten salts, however, even the variation of redox potential depending on various electrolytes has not been well explained scientifically. To obtain the information on the local structure of neodymium cation in various molten electrolytes, the systematic characterization using extended X-ray absorption fine structure (EXAFS) has been carried out.

**EXPERIMENTS:** Since the concentration of neodymium in electrolytes is 1 to 5 molar %, the EXAFS measurements have been carried out using high energy X-ray generated at BL11XU, SPring-8, Japan. The samples of mixture melts have been molten in a quartz vessel kept in an argon circulated glove box and sealed in the quartz cells in a funnel or a rectangular type (X-ray path: 1.5 mm or 10 mm, respectively) under vacuum condition. EXAFS spectra of neodymium K- Edge (43.571 keV) of these samples heated at 923 K by an electric furnace[2] on the beamline have been obtained by a quick scan of transmission mode. The data analyses have been done using WinXAS 3.0[3] and FEFF 8.01[4] and the curve fitting analyses introduced 3<sup>rd</sup> and 4<sup>th</sup> cumulants have been performed since anharmonic oscillation effect cannot be ignored on the spectra at high temperature.

**RESULTS and DISCUSSION:** By utilization of X-ray from an undulator beamline, even such as highly diluted solution with the highly X-ray absorbing element, i.e. NdCl<sub>3</sub>-BaCl<sub>2</sub>-LiCl (1:10:89), could be measured within 5 minutes to obtain decent quality of spectrum. It is epoch making that the similar concentration of the electrolytes will be able to be evaluated by EXAFS. Various structural parameters obtained by assuming 6-coordinated structure for the mixtures of 1 mol % of neodymium in 10 mol % of LiCl exchanged with KCl, CsCl, CaCl<sub>2</sub>, and BaCl<sub>2</sub> are shown in Fig. 1. With reference to the inter-ionic distance between Nd<sup>3+</sup> and Cl<sup>-</sup> in molten pure

LiCl, those with K and Ca do not so much varied but that with Cs gets shorten and that with Ba gets expanded. These tendencies are partly following to the structural information obtained for rare earth trichlorides in various alkali cationic chlorides[5,6]. Although the structural information obtained by EXAFS is limited to the 1<sup>st</sup> coordination sphere around neodymium cation, it is found that even in such diluted solution of neodymium, the local structure has been influenced by the cation existing in 2<sup>nd</sup> coordination sphere from neodymium. The tendency observed in the melts containing Ba<sup>2+</sup> which has larger cationic size is one of the useful informations to explain the anomalous tendencies observed in UV-Vis spectroscopy and electrochemical behaviour[7,8].

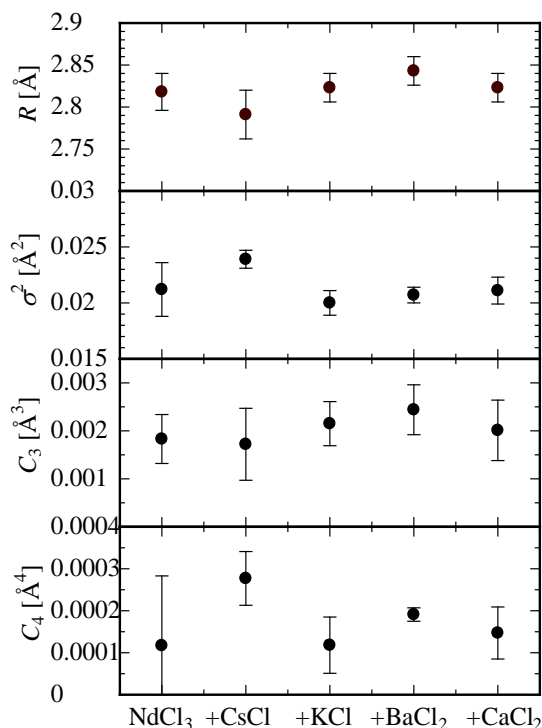


Fig. 1. structure parameters obtained by curve fitting analysis for neodymium in various melts.

### REFERENCES:

- [1] H. Yamana *et al.*, *J. Alloys Compd.*, **408-412** (2006) 66.
- [2] H. Matsuura *et al.*, *J. Alloys Compd.*, **408-412** (2006) 80.
- [3] T. Ressler, *J. Synchrotr. Rad.*, **5** (1998) 118.
- [4] A. L. Ankudinov *et al.*, *Phys. Rev. B*, **58** (1998) 7565.
- [5] Y. Okamoto *et al.*, *J. Synchrotr. Rad.*, **8** (2001) 1191.
- [6] Y. Okamoto *et al.*, *J. Phys. Chem. A*, **114** (2010) 4664.
- [7] K. Fukasawa *et al.*, *J. Nucl. Mater.*, **414** (2011) 265.
- [8] K. Fukasawa *et al.*, *J. Alloys Compd.*, **509** (2011) 5112.

## Electrochemical and Spectroelectrochemical Studies on $[\text{UO}_2\text{Cl}_4]^{2-}$ in 1-Ethyl-3-methylimidazolium Based Ionic Liquids - Identification of Uranyl(V) Species -

T. Ogura and Y. Ikeda

*Research Laboratory for Nuclear Reactors, Tokyo Institute of Technology*

**INTRODUCTION:** Room temperature ionic liquids (ILs) are expected to be useful media for recovering uranium from spent nuclear fuels and solid wastes contaminated with uranium[1], *e.g.*, as media for extraction and electrolytic deposition. Hence, the extraction behavior of uranyl species from aqueous to IL phase, the electrochemical behavior of uranyl species in ILs, and so on have been studied[2-5]. In the present study, we have examined the electrochemical behavior of uranyl(VI) species,  $(\text{EMI})_2\text{UO}_2\text{Cl}_4$ , in the mixture of EMICl and EMIBF<sub>4</sub> (EMI = 1-ethyl-3-methylimidazolium) to obtain the basic data for evaluating application of ILs to pyro-reprocessing process. We used the mixture of EMICl and EMIBF<sub>4</sub> as the reaction media, because this mixture is liquid at room temperature.

**EXPERIMENTS:** 1-Ethyl-3-methylimidazolium chloride and EMIBF<sub>4</sub> were commercially available from Kanto Chemical Co., Inc. The former was repeatedly (at least 4 times) treated with activated charcoal in acetonitrile, followed by filtration and vacuum evaporation, and the latter was used without further purification. The  $[\text{EMI}]_2[\text{UO}_2\text{Cl}_4]$  was prepared by the similar method reported previously. UV-visible absorption spectra of solutions prepared by dissolving  $[\text{EMI}]_2[\text{UO}_2\text{Cl}_4]$  into EMIBF<sub>4</sub>/Cl ( $[\text{Cl}^-] = [\text{BF}_4^-] = 3.54 \times 10^{-1} \text{ M}$ ) were measured by using SHIMADZU UV-3150 spectrophotometer. Cyclic voltammetric (CV) measurements of sample solutions were carried out at 25 °C under a dry Ar atmosphere using BAS ALS660B. A conventional three-electrode system was utilized, *i.e.*, a Pt disc working electrode (surface area (*S*): 0.020 cm<sup>2</sup>), a Pt wire counter electrode and an Ag/Ag<sup>+</sup> reference electrode (0.01 M AgNO<sub>3</sub>, 0.1 M tetra-*n*-butylammonium perchlorate in acetonitrile) connected to the sample solution through a glass frit filled with the solvent ionic liquid. The Fc/Fc<sup>+</sup> couple was used as the reference redox system. All potentials reported here are *versus* Fc/Fc<sup>+</sup>. Dissolved O<sub>2</sub> in the sample solutions was removed by passing Ar gas through for at least 10 min prior to starting the CV measurements. The ohmic drop in this experiment was compensated by

subtracting the cyclic voltammogram of the blank EMIBF<sub>4</sub>/Cl solution from that of  $[\text{UO}_2\text{Cl}_4]^{2-}$  in the same solvent.

**RESULTS:** The cyclic voltammograms of the EMICl and EMIBF<sub>4</sub> mixture dissolved  $[\text{EMI}]_2[\text{UO}_2\text{Cl}_4]$  ( $6.06 \times 10^{-2} \text{ M}$ ) were measured. One redox couple is observed around -1.0 V *vs.* Fc/Fc<sup>+</sup>. It was found that the values of  $(E_{\text{pc}} + E_{\text{pa}})/2$  ( $E_{\text{pc}}$  and  $E_{\text{pa}}$  are peak potentials for cathodic and anodic peaks, respectively) are constant (-0.989 V *vs.* Fc/Fc<sup>+</sup>) regardless of the scan rates, and that a plot of  $i_{\text{pc}}$  (the peak currents of cathodic peaks) against  $v^{1/2}$  gives a linear relationship with slope of 8.21. Furthermore, we estimated the standard rate constant ( $k^0$ ) based on the kinetic parameter ( $\psi$ ) proposed by Nicholson. The  $k^0$  value was estimated as  $(2.7\sim 2.8) \times 10^{-4} \text{ cm/s}$  in the range of scan rates from 50 to 300 mV/s. The estimated value is in the range of the  $k^0$  value ( $(4.0 \sim 9.9) \times 10^{-3} > k^0 > (2.7 \sim 6.6) \times 10^{-7}$ ) for the quasi-reversible reaction on the basis of the reversibility factor (*A*) of Matsuda and Ayabe. These results suggest that the electrochemical reaction of  $[\text{UO}_2\text{Cl}_4]^{2-}$  occurs quasi-reversibly. In order to examine the reduction product, we carried out spectroelectrochemical studies using optically transparent thin layer electrode (OTTLE) cell in the range from 0 to -1.306 V. The isosbestic point is found to be observed around 350 nm. In addition, from the Nernstian plot, the electron stoichiometry (*n*-value) and the formal potential were evaluated as 0.99 and -0.99 V, respectively. These results indicate that  $[\text{U}^{\text{VI}}\text{O}_2\text{Cl}_4]^{2-}$  is reduced to  $[\text{U}^{\text{V}}\text{O}_2\text{Cl}_4]^-$  in the mixture of EMICl and EMIBF<sub>4</sub> and the resulting  $[\text{U}^{\text{V}}\text{O}_2\text{Cl}_4]^-$  species are relatively stable.

### REFERENCES:

- [1] V.A. Cocalia, K.E. Gutowski, and R.D. Rogers, *Coord. Chem. Rev.*, **250**, 755 (2006).
- [2] K. Binnemans, *Chem. Rev.*, **107**, 2592 (2007).
- [3] Y. Ikeda, K. Hiroe, N. Asanuma, and A. Shirai, *J. Nucl. Sci. Technol.*, **46**, 158 (2009).
- [4] Y. Ohashi, N. Asanuma, M. Harada, Y. Wada, T. Matsubara, and Y. Ikeda, *J. Nucl. Sci. Technol.*, **46**, 771 (2009).
- [5] T.J. Bell and Y. Ikeda, *Dalton Trans.*, **40**, 10125 (2011).

T. Goto and K. Hachiya<sup>1</sup>

Department of Environmental Systems Science, Faculty of Science and Engineering, Doshisha University

<sup>1</sup>Department of Fundamental Energy Science, Graduate School of Energy Science, Kyoto University

**INTRODUCTION:** Molten salts are promising media for separation and recovery of the spent nuclear fuel. To realize the process, clarifying the physicochemical properties of f-elements in molten salts is required. Although cesium is known as an important fission product, little has been reported about its effect on the molten salts. From the background, we have examined the influence that the existence of the cesium ion gave to other multi valence ions in molten LiCl-KCl. In this report, aluminum ion was selected as model of a multi valence cation (f-elements) and electrochemical behavior of aluminum ion in molten LiCl-KCl and LiCl-KCl-CsCl were investigated.

**EXPERIMENTS:** The LiCl-KCl-CsCl eutectic (LiCl-KCl-CsCl=57.5:13.3:29.2 mol %) was used as an electrolyte. AlCl<sub>3</sub> was directly added to the melt as an Al(III) ion source. A Chromel-Alumel thermocouples were used for temperature measurement. The temperature was maintained within 1±K by a temperature control unit. All experiments were conducted in an argon atmosphere with a continuous gas refining instrument. A tungsten wire electrode covered with a high purity alumina tube was used as a working electrode for investigating electrochemical behavior of aluminum ions. The reference electrode was a silver wire immersed in LiCl-KCl-CsCl containing 1 mol% of AgCl, placed in a Pyrex glass tube with a thin bottom to maintain electrical contact with the melt. The potential of this reference electrode was calibrated with reference to that of a Li<sup>+</sup>/Li electrode, which was prepared by electrodepositing Li metal on W wire. All potentials are given in reference to Li<sup>+</sup>/Li electrode potential. A potentiogalvanostat was used for electrochemical measurement. Diffusion coefficient of aluminum ions was determined by means of electrochemical measurement. Micro Raman measurement was performed for analyzing the liquid structure and coordination of aluminum ion in molten salts.

**RESULTS:** Figure 1 shows a typical cyclic voltammograms (CV) obtained at 0.1 Vs<sup>-1</sup> in the eutectic LiCl-KCl-CsCl melt containing Al(III) ions on a tungsten electrode. The peaks A and A' are attributed to the reduc-

tion of Al(III) to Al and the oxidation of Al to Al(III) respectively.

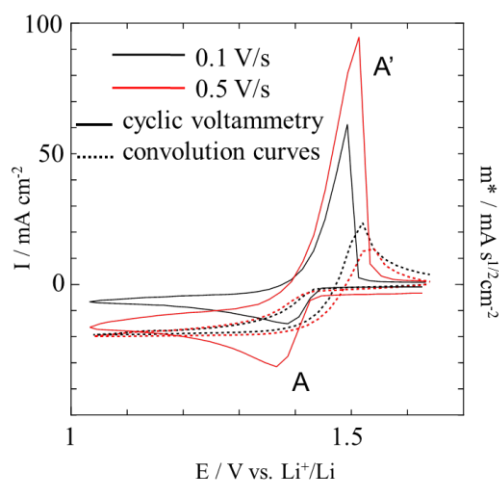


Detail analysis of the voltammogram CV was performed by using the convolution analysis as shown in Fig.1. By analyzing the convoluted curves, it can be observed that the direct and reverse scans are not identical. This indicated that the reduction of Al(III) on a tungsten electrode was not reversible reaction and the electrochemical couple of Al(III)/Al was typically characteristic of a soluble-insoluble exchange.

According to the theory of convolution, the diffusion coefficient is calculated using the equation(3):

$$m^* = nFCD^{0.5} \quad (3)$$

where  $m^*$  is the limiting current of the convoluted curve of the corresponding cyclic voltammogram. The diffusion coefficient of Al(III) in LiCl-KCl-CsCl at 603 K was estimated to be  $4.0 \times 10^{-8} \text{ cm}^2 \text{ s}^{-1}$ . The diffusion coefficient was 3 orders lower than that in LiCl-KCl. This implied the coordination of aluminum ion in the molten salts was affected by the existence of the cesium ion. These results were also supported by the Raman spectra of aluminum ion which largely changed greatly by the presence of cesium ions.



#### REFERENCES:

- [1] Patrick Masset et al., Journal of Nuclear Materials, 344, pp.173-179 (2005)



S. Nakamura, F. Kitatani, H. Harada  
T. Fujii<sup>1</sup>, A. Uehara<sup>1</sup> and H. Yamana<sup>1</sup>

Japan Atomic Energy Agency  
<sup>1</sup>Research Reactor Institute, Kyoto University

**INTRODUCTION:** As a part of the research projects, a series of cross-section measurements has been carried out for minor actinides to obtain basic data for studies on nuclear-fuel cycles and nuclear transmutation. Neptunium-237 is one of important isotopes because it contributes to the long-term radiotoxicity of nuclear wastes. However, there still exist large discrepancies among reported data of the thermal-neutron capture cross section ( $\sigma_0$ ) as shown in **Figure 1**. Then, the present work reports the measurement for the thermal-neutron capture cross-section of  $^{237}\text{Np}$ .

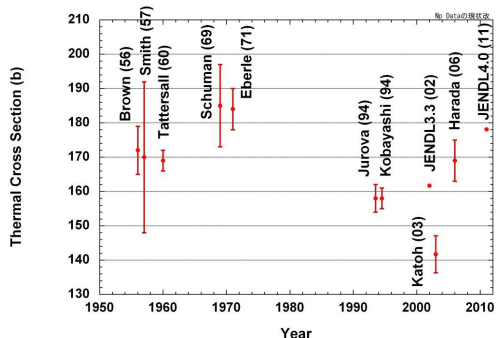


**Fig.1.** Situation of the reported data of  $\sigma_0$  for  $^{237}\text{Np}$

**EXPERIMENT:** A standardized solutions of  $^{237}\text{Np}$  (200Bq) were irradiated together with neutron monitors in the pneumatic tube (Pn-2) of the KUR in the latter half of 2010. The reactor power was 1 MW. The  $^{237}\text{Np}$  samples were irradiated for 600sec, and another one together with a Gd shield (25 $\mu\text{m}$  in thickness) for 300 sec. After the irradiations, induced activities of samples were measured with a high purity Ge detector. **Figure 1** shows the neutron fluxes obtained from the measurements of the irradiated neutron monitors. The thermal neutron flux was  $4.4 \times 10^{12}$  n/cm<sup>2</sup>sec at the irradiation position of the Pn-2.

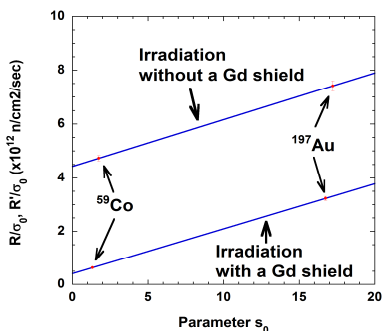


**Fig.2.** neutron flux components at Pn-2

**ANALYSIS AND DISCUSSION:** The reaction rates of  $^{237}\text{Np}$  samples were calculated with  $\gamma$ -ray yields, efficiencies, decay data and  $\gamma$ -ray emission probabilities. However, there are still discrepancies among the data of the  $\gamma$ -ray emission probabilities ( $I_\gamma$ ). The data of the emission probability for 984-keV  $\gamma$ -ray emitted from  $^{238}\text{Np}$  have been reported as shown in **Table 1**. These data are in good agreement with each other.

**Table 1** 984-keV  $\gamma$ -ray emission probability

Author	Year	984-keV $I_\gamma$ (%)
Harada <i>et al.</i>	2006	$25.2 \pm 0.5$
Rengan <i>et al.</i>	2006	$25.2 \pm 0.5$
Chang <i>et al.</i>	1990	$25.19 \pm 0.21$
Lederer	1981	27.8
Winter <i>et al.</i>	1972	25.4

On the other hand, there are still discrepancies among reported data of  $I_\gamma$  for 984-keV  $\gamma$ -ray emitted from  $^{233}\text{Pa}$  as listed in **Table 2**.

**Table 2.** 312-keV  $\gamma$ -ray emission probability

Author	Year	312-keV $I_\gamma$ (%)
Harada <i>et al.</i>	2006	$41.6 \pm 0.9$
Singh and Tuli	2005	$38.5 \pm 0.4$
Schukin <i>et al.</i>	2004	$37.5 \pm 0.24$
Lucva <i>et al.</i>	2000	$37.8 \pm 0.6$
Woods <i>et al.</i>	2000	$38.7 \pm 0.4$
Gehrke <i>et al.</i>	1979	$38.6 \pm 0.5$

Then, when the combinations of  $I_\gamma$  data were changed, their influences on the  $\sigma_0$  were examined. When the influences were examined about the data by Kobayashi and Katoh, their results are modified as shown in **Table 3**.

**Table 3.** influences on the  $\sigma_0$  by the  $I_\gamma$  data

Author	Pa: 38.6%	41.6	38.5
	Np: 27.8%	25.2	25.2
This Work	-	$198 \pm 8$	$183 \pm 7$
Katoh('03)	$141.7 \pm 5.4$	$169 \pm 6$	$156 \pm 6$
Kobayashi('94)	$158 \pm 3$	$196 \pm 4$	$181 \pm 3$

The present work is in good agreement with the data by Kobayashi. From reviewing data, the discrepancies among the  $\sigma_0$  of  $^{237}\text{Np}$  would be caused by the  $I_\gamma$  data used for the analyses. The data of the  $\sigma_0$  should be settled by experimental further check on the  $I_\gamma$  data.